

An Intelligent PSO-based Topology Control Protocol for Wireless Sensor Networks

Arash Nikdel¹, Mahdi Mosleh² and Hagar Noori³

^{1,2,3} *Department of Computer Engineering, Andimeshk Branch, Islamic Azad University, Andimeshk, Iran*

nikdelarash@yahoo.com¹, mahdi_mosleh@yahoo.com², hagar_noori@yahoo.com³

Abstract

Topology control protocols try to decrease the average of node's transition radius without decreasing network connectivity. In this paper, we propose a new Particle Swarm Optimization-based Topology Control protocol for wireless sensor networks called PSOTC. In this protocol, proper transition radius can be determined using Particle Swarm Optimization (PSO) algorithm. The proposed protocol dynamically adjusts transition radius of nodes (unlike previous protocols which should select radius values from among predefined values). Thus, the proposed protocol has some advantages compared to the previous protocols. PSOTC protocol has less average number of neighbors compared to the existing protocols. Also, the energy consumption in our protocol is less than other protocols and the network lifetime will be prolonged. In addition, the network connectivity in our protocol is in the acceptable level. The proposed protocol is simulated and the above advantages are demonstrated by the simulation results.

Keywords: *Wireless Sensor Networks, Topology Control, Particle Swarm Optimization algorithm, Network Lifetime, Energy Consumption*

1. Introduction

Recent technological advances have led to the emergence of small, low-power devices which integrate sensors with limited processing and wireless communication capabilities [1]. The wireless sensor network (WSN) has emerged as a promising tool for monitoring the physical world and has a wide variety of potential applications in many fields [2, 3]. Sensors can be deployed rapidly and cheaply, thereby enabling large-scale, on-demand monitoring and tracking [2]. Wireless sensor networks open a wide range of applications, including environment monitoring, disaster prediction, military surveillance and vehicle tracking [1, 2]. Topology control in wireless sensor networks constructs an optimized network topology structure to satisfy the application requirements, such as network connectivity and coverage [1]. Choosing appropriate topology for a sensor network has so much effect on networks' performance, especially considering power consumption and lifetime of the network [4]. In this paper, we propose a new Particle Swarm Optimization-based Topology Control protocol for wireless sensor networks called PSOTC¹. In this protocol, proper transition radius can be determined using Particle Swarm Optimization (PSO) algorithm. The proposed protocol dynamically adjusts transition radius of nodes. Thus, the proposed protocol has some advantages compared to previous protocols. These advantages are demonstrated by the simulation results. The remaining of this paper is organized as follow: Related works are

¹ Particle Swarm Optimization-based Topology Control

explained in section 2. In section 3 the problem definition is introduced. Proposed protocol is explained in section 4. Simulation results are shown in section 5 and a final conclusion is discussed in Section 6.

2. Related Works

So far, many protocols have been introduced for topology control in sensor networks. Topology control protocols are divided into homogeneous and heterogeneous topology control protocols [4]. In homogeneous topology control, all network nodes use the same transition radius and topology control problem is to find a minimum value for transition radius considering the network characteristics such as network connectivity and coverage [4]. In heterogeneous topology control, the network nodes can have non uniform transition radius [4]. In this group, the protocols with information used for making topology are divided into three subgroups. The first subgroup consists of methods based on location. In this subgroup, nodes are informed of their location. R&M² [5] and LMST³ [6] are two examples of these methods. The second subgroup consists of the methods based on orientation. In these methods, nodes don't have exact information of their location, but they can identify the direction of their neighbors. CBTC⁴ [7] is an example of these methods. The third subgroup consists of the methods based on neighbors. In these methods, nodes have limited information about their neighbors. This information consists of ID number, and distance or quality of node's neighbors. XTC⁵ [8] and Kneigh⁶ [9] are examples in this subgroup.

RAA-2L⁷ is another topology control protocol. In this protocol, each node chooses one of two transition radius R_S or R_W ($R_W < R_S$) [10]. If a node with transition radius R_W could communicate with a neighbor with transition radius R_S , it chooses the transition radius R_W , else it chooses the transition radius R_S . In RAA-3L⁸, each node chooses one of three transition radius: R_t , R_S or R_W ($R_W < R_t < R_S$). In our previous work [11], we proposed a Genetic Algorithm-based Topology Control protocol for wireless sensor networks called GATC⁹, but the overhead of GATC is heavy, since GATC uses many messages for determining the proper transition radii.

3. The Network Model and the Assumptions

In this section, we present the model and the assumptions used in this paper.

3.1. Adjustable Transition Radius

We assume that each node has adjustable transition radius which can be between a minimum and a maximum transition radius. R_{min} is the transition radius with minimum power, R_{max} is the transition radius with maximum power and R_T is the selective transition radius of node. The value of R_T should be between the R_{min} and R_{max} ($R_{min} \leq R_T \leq R_{max}$). The values of transition radius R_{min} and R_{max} will be calculated based on R_t , the value of transition radius R_t .

² Rodoplu and Ming

³ Local Minimum Spanning Tree

⁴ Cone Based Topology Control Protocol

⁵ Extreme Topology Control

⁶ k -neighbors

⁷ Radius Adaptation Algorithm-2 Level

⁸ Radius Adaptation Algorithm-3 Level

⁹ Genetic Algorithm-based Topology Control protocol

is determined proportional to the network density [12]. When the distance between 2 nodes is less than R_{max} , we assume they are neighbor. Each node has three different neighbor sets. The sets of A_{min} , A_T and A_{max} are obtained by Eq. (1). In Eq. (1), $A_X(N)$ shows the A_X set for node N , n_i is the neighbor's node number, and D_{ni} is the distance between current node and n_i .

$$\begin{aligned} n_i \in A_{min}(N) & \quad \text{if } D_{ni} \leq R_{min} \\ n_i \in A_T(N) & \quad \text{if } R_{min} < D_{ni} \leq R_T \\ n_i \in A_{max}(N) & \quad \text{if } R_T < D_{ni} \leq R_{max} \end{aligned} \quad (1)$$

Therefore, for each node N we have Eq. (2) and Eq. (3):

$$A_{max}(N) \cup A_T(N) \cup A_{min}(N) = \text{All neighbors of node } N \quad (2)$$

$$A_{max}(N) \cap A_T(N) \cap A_{min}(N) = \varnothing \quad (3)$$

The main problem in this study is choosing minimum transition radius R_T between R_{min} and R_{max} for each node without decreasing the network connectivity.

3.2. The cluster-based Architecture

Similar to the cluster-based coverage control scheme introduced in [13], we use a cluster-based topology control scheme in this paper, which is scheduled into some rounds. In each round, first the target area is divided into several equal squares. Then the node in each square having the largest energy will be chosen as the cluster-head, and the procedure of selecting the cluster-head is the same as the method in [14]. Each cluster-head has full control of the square and it will choose transition radius of nodes. In the following round, another sensor set will be selected as the cluster head. So the energy consumption among all the sensors can be balanced totally.

3.3 Energy consumption analysis

To summarize the energy consumption analysis, here we only consider the energy consumed by the transmission function, and don't include the power consumption of sensing and calculation [13]. Assume that the size of the monitoring area is A_{area} , the working sensor set is $S = \{\hat{n}_1, \hat{n}_2, \dots, \hat{n}_n\}$ and the transition radius set is $R_T = \{R_{T1}, R_{T2}, \dots, R_{Tn}\}$, where R_{Ti} is the transition radius of node \hat{n}_i , and $R_{Ti} \in [R_{min}, R_{max}]$.

According to different energy consumption models, the energy consumed by a node to deal with a transmission task is proportional to r^2 or r^4 , where r is the transition radius of the node [15]. In this paper, we take the transmission energy consumption as Eq. (4), where u is the impact factor which its value is near 1:

$$E(r) = u \cdot r^2 \quad (4)$$

Thus, the energy consumption of the sensor set, which is related to the sum of the sensor's transition radius squared, is defined as Eq. (5) [13]:

$$E_{total} = E(R_T) = \sum_{i=1}^n E(R_{Ti}) = \sum_{i=1}^n u \cdot R_{Ti}^2 = u \cdot \sum_{i=1}^n R_{Ti}^2 \quad (5)$$

So, the energy consumption per area is given as Eq. (6):

$$E_{per-Area} = E_{total} / A_{area} = u \cdot \sum_{i=1}^n R_{Ti}^2 / A_{area} \quad (6)$$

3.4 The complete connectivity of the sensor network

In this paper, we will deal with the nodes deployed randomly. Assume that each one knows its own location which can be achieved by using some location systems [16]. A WSN can be modeled as a graph $G=(V, E)$, where V is the set of sensor nodes and E is the set of wireless links [17]. The complete connectivity of the sensor network means the ability of communicating with all the network nodes. Thus, we will define the complete connectivity of the sensor network, C , as Eq. (7):

$$\begin{aligned} \text{If } MCP = n \text{ Then } C &= 1 \\ \text{Else } C &= \varepsilon \end{aligned} \quad (7)$$

In (7), MCP is the biggest connected component of the sensor network and n is the number of sensor nodes. Also ε shows a very small positive number. Thus, we will define the probability of the complete connectivity, P_C , as Eq. (8):

$$P_C = \sum_{i=1 \text{ to } N_d} C_i / N_d \quad (8)$$

In (8), N_d is the number of different configuration of network nodes.

4. Proposed Protocol

In this section, we try to decrease average of node's transition radius without decreasing the network connectivity. It can be supposed that the transition radius of each node changes with a special velocity. In proposed algorithm, at first the primary population of nodes transition radius are selected randomly. Also for each node a variation velocity of transition radius is selected randomly. Then the objective function for the transition radius set is evaluated and based on this evaluation, the variation velocity of the nodes transition radius changes.

Regarding all transition radii which each node has had it by now, there is a best one for it. This transition radius for each node is the one who has the best value of objective function in comparison with its all former transition radii. The best transition radius for each node $n_i \in S = \{n_1^{\wedge}, n_2^{\wedge}, \dots, n_n^{\wedge}\}$ is called the Personal Best Transition Radius which is abbreviated as $R_{T-Pbest\ i}^{\wedge}$. Thus, we perform a Personal Best Transition Radius Set, $R_{T-Pbest}$, as Eq. (9):

$$R_{T-Pbest} = (R_{T-Pbest\ 1}^{\wedge}, R_{T-Pbest\ 2}^{\wedge}, R_{T-Pbest\ 3}^{\wedge}, \dots, R_{T-Pbest\ n}^{\wedge}) \quad (9)$$

Also, the best transition radius set which the sensor set has had by now is called the Global Best Transition Radius with the abbreviation $R_{T-Gbest}$ and are shown as Eq. (10):

$$R_{T-Gbest} = (R_{T-Gbest\ 1}^{\wedge}, R_{T-Gbest\ 2}^{\wedge}, R_{T-Gbest\ 3}^{\wedge}, \dots, R_{T-Gbest\ n}^{\wedge}) \quad (10)$$

The main loop of algorithm continues until the number of its repeats exceeds the threshold value or the objective function becomes better than the threshold value. Therefore, the proposed algorithm includes ten steps as follow:

Phase1. The problem and the algorithm parameter initialization:

Step 1: Initializing A_{min} , A_T and A_{max} sets for each node.

Step 2: Producing the lower bound and the upper bound of the transition radius for each node.

Step 3: Calculating the Personal Objective Function value for transition radius of each node, $f_P(R_T^{\wedge} i)$.

Step 4: Initializing each node's transition radius, $R_T^{\wedge} i$, and also the velocity of its variation $v_T^{\wedge} i$ randomly.

Step 5: Considering $R_{T_i}^{\wedge}$ as the initial value for the best transition radius of node, $R_{T-Pbest_i}^{\wedge}$, and also R_T as the initial value for the best transition radius of the sensor set, $R_{T-Gbest}$.

Phase2. Repeating the main loop of algorithm until meeting the termination criteria:

Step 6: Considering the n -dimensional r_1 and r_2 vectors as the transition radius set, R_T . Their values are random numbers between $[0, 1]$.

Step 7: Updating the node's transition radius, $R_{T_i}^{\wedge}$, and also the velocity of the nodes transition radius changes, $v_{T_i}^{\wedge}$, as Eq. (11) and Eq. (12):

$$v_{T_i}^{\wedge new} = w v_{T_i}^{\wedge} + c_1 r_1 (R_{T-Pbest_i}^{\wedge} - R_{T_i}^{\wedge}) + c_2 r_2 (R_{T-Gbest}^{\wedge} - R_{T_i}^{\wedge}) \quad i=1,2, \dots, n \quad (11)$$

$$R_{T_i}^{\wedge new} = R_{T_i}^{\wedge} + v_{T_i}^{\wedge} \quad i=1,2, \dots, n \quad (12)$$

Step 8: evaluating the Global Objective Function value for the transition radius of the sensor set, $f_G(R_T)$.

Step 9: Updating the best transition radius for each node, $R_{T-Pbest_i}^{\wedge}$, and the best transition radius of the sensor set, $R_{T-Gbest}$ according to Eq. (13) and Eq. (14):

$$\forall n_i \in S = \{n_1^{\wedge}, n_2^{\wedge}, \dots, n_n^{\wedge}\} : \text{If } f_P(R_{T-Pbest_i}^{\wedge}) < f_P(R_{T_i}^{\wedge}) \Rightarrow R_{T-Pbest_i}^{\wedge} \leftarrow R_{T_i}^{\wedge} \quad (13)$$

$$\text{If } f_G(R_{T-Gbest}) < f_G(R_T) \Rightarrow R_{T-Gbest} \leftarrow R_T \quad (14)$$

Step 10: Checking the loop termination criteria and jumping to step 6.

In next sections, we describe the proposed algorithm in detail.

4.1 Step 1: Initializing A_{min} , A_T and A_{max} sets for each node.

At first, according to Eq. (15), the transition radius of each node is set between R_{min} and R_{max} .

$$\forall R_{T_i}^{\wedge} \in R_T = (R_{T_1}^{\wedge}, R_{T_2}^{\wedge}, \dots, R_{T_n}^{\wedge}) : R_{T_i}^{\wedge} \leftarrow R_i \quad (15)$$

4.2 Step 2: Calculating the lower bound and the upper bound of the transition radius for each node.

The process of calculating the lower bound and the upper bound of the transition radius for each node $n_i \in S = \{n_1^{\wedge}, n_2^{\wedge}, \dots, n_n^{\wedge}\}$ is as follow:

At first, according to equation (1) as mentioned before, A_{min} , A_T and A_{max} sets are created for all nodes. Then, A_{min} , A_T and A_{max} sets are updated for node n_i . For this purpose, according to Eq. (16), whenever one node of $A_T(n_i)$ and $A_{max}(n_i)$ sets is accessible through the nodes which are in $A_{min}(n_i)$ set, that node will be removed from these sets and will be added to $A_{min}(n_i)$ set. Also, whenever one node of $A_{max}(n_i)$ sets is accessible through the nodes which are in $A_T(n_i)$ set, that will be removed from $A_{max}(n_i)$ set and will be added to $A_T(n_i)$ set:

$$n_i \in S = \{n_1^{\wedge}, n_2^{\wedge}, n_3^{\wedge}, \dots, n_n^{\wedge}\}; \quad (16)$$

$$\begin{aligned} &\forall n_x \in A_{min}(n_i) \exists n_y \in A_{min}(n_x) \text{ AND} \\ &\quad (n_y \in A_T(n_i) \text{ OR } n_y \in A_{max}(n_i)) \Rightarrow \\ &\quad \begin{cases} A_{min}(n_i) = A_{min}(n_i) + n_y \\ A_T(n_i) = A_T(n_i) - n_y \text{ OR } A_{max}(n_i) = A_{max}(n_i) - n_y \end{cases} \\ &\forall n_x \in A_T(n_i) \exists n_y \in A_{min}(n_x) \text{ AND } n_y \in A_{max}(n_i) \Rightarrow \\ &\quad \begin{cases} A_T(n_i) \leftarrow A_T(n_i) + n_y \\ A_{max}(n_i) \leftarrow A_{max}(n_i) - n_y \end{cases} \end{aligned}$$

In (16), $A_X(n_i)$ shows the A_X set of node n_i . Then, regarding the $A_T(n_i)$ and $A_{max}(n_i)$ conditions, we determine the transition radius range for node n_i . The method of determining the transition radius range is calculated according to the four conditions presented in Eq. (17):

$$n_i \in S = \{\hat{n}_1, \hat{n}_2, \hat{n}_3, \dots, \hat{n}_n\}; \quad (17)$$

If $A_T(n_i) = \varphi$ AND $A_{max}(n_i) = \varphi$ Then	$R_{range \hat{i}} = [R_{min}, R_{min}]$
Else If $A_T(n_i) \neq \varphi$ AND $A_{max}(n_i) = \varphi$ Then	$R_{range \hat{i}} = [R_{min}, R_{T \hat{i}}] = [R_{min}, R_l]$
Else If $A_T(n_i) \neq \varphi$ AND $A_{max}(n_i) \neq \varphi$ Then	$R_{range \hat{i}} = [R_{T \hat{i}}, R_{max}] = [R_l, R_{max}]$
Else If $A_T(n_i) \neq \varphi$ AND $A_{max}(n_i) \neq \varphi$ Then	$R_{range \hat{i}} = [R_{min}, R_{max}]$

Thus, we find a transition radius ranges set, R_{ranges} , as Eq. (18):

$$Transition \ Radius \ Ranges \ set = R_{range} = \{R_{range \hat{1}}, \dots, R_{range \hat{n}}\}; R_{range \hat{i}} = [R_{low \hat{i}}, R_{up \hat{i}}] \quad (18)$$

Now, the transition radius of each node can be only within its determined range.

4.3 Step 3: Evaluating the Personal Objective Function for the transition radius of each node, $f_P(R_{T \hat{i}})$:

In this step, we define the Personal Objective Function for the transition radius of each node, $f_P(R_{T \hat{i}})$. According to equation (4), in energy consumption model, the energy consumed by a node to deal with a transition task relates to the node transition radius squared. So, the $f_P(r)$ function value is defined as stated in Eq. (19):

$$f_P(r) = 1 / (r + \gamma) \quad (19)$$

Where γ shows very small positive number and is selected as the function value which doesn't exceed a given limit. The process of calculating $f_P(R_{T \hat{i}})$ function value for each node $n_i \in S = \{\hat{n}_1, \hat{n}_2, \dots, \hat{n}_n\}$ is as Eq. (20):

$$\forall n_i \in S = \{\hat{n}_1, \hat{n}_2, \dots, \hat{n}_n\}; R_{T-Pbest \hat{i}} \leftarrow R_{low \hat{i}} \quad (20)$$

Therefore we have Eq. (21):

$$\forall n_i \in S = \{\hat{n}_1, \hat{n}_2, \dots, \hat{n}_n\}; f_P(n_i) = f_P(R_{T-Pbest \hat{i}}) = f_P(R_{low \hat{i}}) = 1 / (R_{low \hat{i}} + \gamma) \quad (21)$$

4.4 Step 4: Initializing each node's transition radius, $R_{T \hat{i}}$, and also the velocity of its variations, $v_{T \hat{i}}$, randomly.

In this step, each node transition radius, $R_{T \hat{i}}$, and also the velocity of its variations, $v_{T \hat{i}}$, is initialized randomly according to Eq. (22) and Eq. (23)

$$\forall R_{T \hat{i}} \in R_T = (R_{T \hat{1}}, R_{T \hat{2}}, \dots, R_{T \hat{n}}); R_{T \hat{i}} = random \ number \ between \ [R_{low \hat{i}}, R_{up \hat{i}}] \quad (22)$$

$$\forall v_{T \hat{i}} \in v_T = (v_{T \hat{1}}, v_{T \hat{2}}, \dots, v_{T \hat{n}}); v_{T \hat{i}} = random \ number \ between \ [v_{low}, v_{up}] \quad (23)$$

4.5 Step 5: Considering $R_{T \hat{i}}$ as the initial value for the best transition radius of node, $R_{T-Pbest \hat{i}}$, and also R_T as the initial values for the best transition radius of the sensor set, $R_{T-Gbest}$.

In this step, we consider $R_{T \hat{i}}$ as the initial value for the best transition radius of node, $R_{T-Pbest \hat{i}}$. It is shown in Eq. (24):

$$\forall R_{T-Pbest \hat{i}} \in R_{T-Gbest} = (R_{T-Gbest \hat{1}}, R_{T-Gbest \hat{2}}, \dots, R_{T-Gbest \hat{n}}); R_{T-Pbest \hat{i}} \leftarrow R_{T \hat{i}} \quad (24)$$

Also, we consider $R_T = (R_{T1}, R_{T2}, \dots, R_{Tn})$ as the initial values for the best transition radius of the sensor set, $R_{T-Gbest}$. It is shown in Eq. (25)

$$R_{T-Gbest} = (R_{T-Gbest1}, R_{T-Gbest2}, \dots, R_{T-Gbestn}) \leftarrow R_T = (R_{T1}, R_{T2}, \dots, R_{Tn}) \quad (25)$$

4.6. Step 6: Considering n -dimensional r_1 and r_2 vectors as the transition radius set, R_T . Their value is a random number between [0,1].

We Consider n -dimensional r_1 and r_2 vectors for which the values are random numbers between [0,1]. These vectors are presented as Eq. (26) and Eq. (27):

$$\forall r_{1i} \in r_1 = \{ r_{11}, r_{12}, \dots, r_{1n} \} : r_{1i} = \text{random numbers between } [0,1] \quad (26)$$

$$\forall r_{2i} \in r_2 = \{ r_{21}, r_{22}, \dots, r_{2n} \} : r_{2i} = \text{random numbers between } [0,1] \quad (27)$$

4.7. Step 7: Updating the nodes' transition radius, R_{Ti} , and also the velocity of the nodes' transition radius variations, v_{Ti} .

In this step, we update the nodes transition radius, R_{Ti} , and also the velocity of the nodes transition radius variations, v_{Ti} , as Eq. (28) and Eq. (29):

$$v_{Ti}^{new} = w v_{Ti} + c_1 r_{1i} (R_{T-Pbest_i} - R_{Ti}) + c_2 r_{2i} (R_{T-Gbest_i} - R_{Ti}) \quad i=1, 2, \dots, n \quad (28)$$

$$R_{Ti}^{new} = R_{Ti} + v_{Ti} \quad i=1, 2, \dots, n \quad (29)$$

The transition radius of each node $n_i \in S = \{n_1, n_2, \dots, n_n\}$ can be only within its determined range $R_{range_i} = [R_{low_i}, R_{up_i}]$ according to Eq. (30):

$$\text{If } R_{Ti}^{new} \geq R_{up_i} \text{ Then } R_{Ti} \leftarrow \min(R_{Ti}^{new}, R_{up_i}) \quad i=1, 2, \dots, n \quad (30)$$

$$\text{Else } R_{Ti}^{new} = R_{Ti} \leftarrow \max(R_{low_i}, R_{Ti}^{new})$$

4.8. Step 8: Evaluating the Global Objective Function value for the transition radius of the sensor set, $f_G(R_T)$.

In this step, we evaluate the Global Objective Function value for the transition radius of the sensor set, $f_G(R_T)$. Considering that in the energy consumption model, the energy consumed by a node to deal with a transition task relates to the node transition radius squared as stated in Eq. (31):

$$E(R_{Ti}) = u \cdot R_{Ti}^2 \quad (31)$$

So, the f_G function is defined as stated in Eq. (32):

$$f_G(R_T) = C / E(R_T) = C / (\sum_{i=1 \text{ to } n} E(R_{Ti})) = C / (u \cdot \sum_{i=1 \text{ to } n} (R_{Ti})^2) \quad (32)$$

Where, C indicates the complete connectivity of the sensor network.

4.9. Step 9: Updating the best transition radius for each node, $R_{T-Pbest_i}$, and the best transition radius of the sensor set, $R_{T-Gbest}$.

In this step, we update the best transition radius for each node, $R_{T-Pbest_i}$, and the best transition radius of the sensor set, $R_{T-Gbest}$ according to Eq. (33) and Eq. (34):

$$\forall n_i \in S = \{n_1, n_2, \dots, n_n\} : \text{If } f_P(R_{T-Pbest_i}) < f_P(R_{Ti}) \Rightarrow R_{T-Pbest_i} \leftarrow R_{Ti} \quad (33)$$

$$\text{If } f_G(R_{T-Gbest}) < f_G(R_T) \Rightarrow R_{T-Gbest} \leftarrow R_T \quad (34)$$

4.10. Step 10: Checking the loop termination criteria and jumping to step 6

The main loop of the algorithm (steps 6, 7, 8, and 9) continues until meeting one of the conditions stated below:

- The number of performing the main loop of the algorithm exceeds the Threshold Cycles (TI) value.
- The Global Objective Function value for the best global transition radius, $f_G(R_{T-Gbest})$, becomes better than the Threshold value, and also $R_{T-Gbest}$ can provide the complete connectivity of the sensor network. Threshold value is calculated according to Eq. (35):

$$\forall R_{T-Gbest\ i} \in R_{T-Gbest} = \{R_{T-Gbest\ 1}, R_{T-Gbest\ 2}, \dots, R_{T-Gbest\ n}\} : R_{T-Gbest\ i} = R_{low\ i} \Rightarrow f_G(R_{T-Gbest}) \text{ is minimized} \quad (35)$$

After terminating the main loop of the algorithm, the $R_{T-Gbest}$ set is assigned to R_T set according to Eq. (36) and it is the answer of the algorithm:

$$\forall n_i \in S = \{n_1, n_2, \dots, n_n\} : R_{T\ i} \leftarrow R_{T-Gbest\ i} \quad (36)$$

5. Simulation Results

In this section, our proposed protocol is simulated and compared to RAA-2L, RAA-3L [10], and HOM¹⁰ [12] using NS2 simulator.

5.1. Simulation Environment

We considered $500 \times 500\ m^2$ area for these simulations. We deploy the sensor nodes randomly in the target area. The number of sensor nodes, n , in different configurations is considered from 50 to 250 sensor nodes. Each node has a transition range between R_{min} and R_{max} . R_{min} and R_{max} transition radius are considered $0.8 \times R_t$ and $1.25 \times R_t$, respectively. Fig. 1 and Table 1 represent the R_t , R_{min} and R_{max} transition values for different configurations of the sensor network. The threshold value for the number of performing the main loop of the algorithm considered 300 (TI=300). The parameters values for simulation are shown in Table 2. The results mentioned in next sections show the average of performing protocols for one hundred random deployments.

¹⁰ Homogeneous Mode

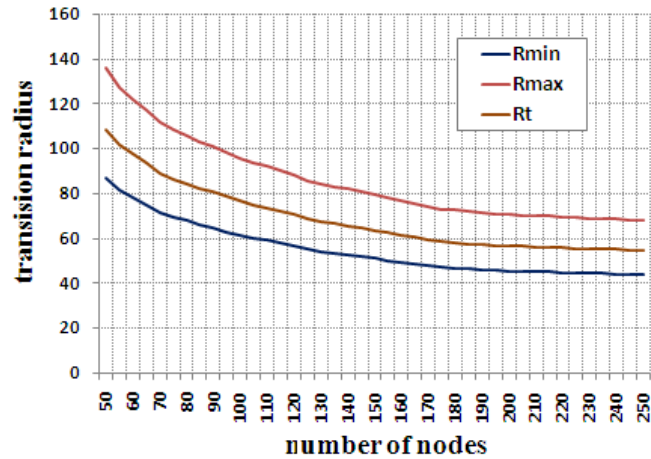


Figure 1. The transition radius values for different configurations of the sensor network

Table 1. The transition radius values for different configurations of the sensor network

Number of nodes (N)	<i>R min</i>	<i>R t</i>	<i>R max</i>
50 node	87.2	109	136
60 node	78.4	98.0	123
70 node	71.6	89.5	112
80 node	68.0	85.0	106
90 node	64.8	81.0	101
100 node	61.6	77.0	96.3
110 node	59.2	74.0	92.5
120 node	56.8	71.0	88.8
130 node	54.4	68.0	85.0
140 node	52.8	66.0	82.5
150 node	51.2	64.0	80.0
160 node	49.6	62.0	77.5
170 node	48.0	60.0	75.0
180 node	46.8	58.5	73.1
190 node	46.0	57.5	71.9
200 node	45.6	57.0	71.3
210 node	45.3	56.6	70.8
220 node	45.0	56.2	70.3
230 node	44.6	55.8	69.8
240 node	44.3	55.4	69.3
250 node	44.0	55.0	68.8

Table 2. The parameters values for simulation

Parameter	ϵ	u	γ	Nd	TI
Value	0.001	1	0	100	300

Three metrics are used for evaluations. These metrics are: the average of transition radius, the average number of neighbors, and the probability of the complete connectivity.

5.2. Comparison with other protocols

In the first experiment, we measured the average of transition radius for PSOTC, RAA-2L, RAA-3L and HOM protocols. The purpose of this experiment is to evaluate the ability of the proposed protocol to decrease the average of transition radius. Note that, in MIN-RANGE, all

of nodes have minimum transition radius (R_{min}). Also, in MAX-RANGE, all of nodes have maximum transition radius (R_{max}). The result of this simulation is depicted in Fig. 2 and Table 3. As can be seen, PSOTC has less average of transition radius and HOM has maximum average of transition radius. Note that, against former protocols, the proposed protocol doesn't use a predetermined transition radius.

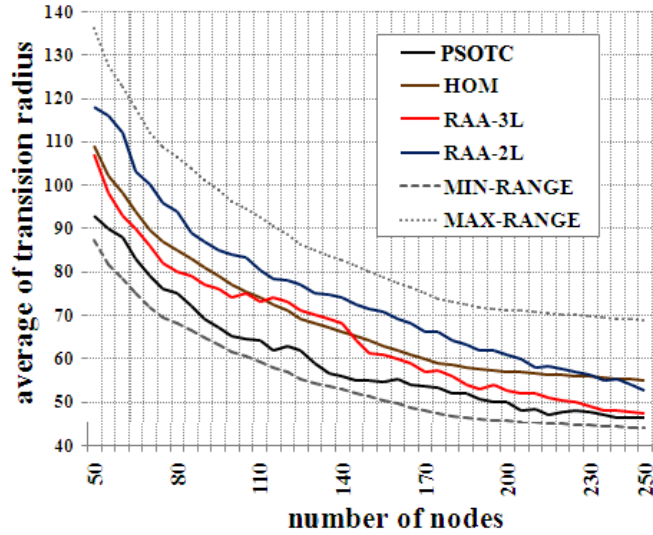


Figure 2. The average of transition radius

Table 3. The average of transition radius

Number of nodes (N)	<i>min-range</i>	<i>HOM</i>	<i>RAA-2L</i>	<i>RAA-3L</i>	<i>PSOTC</i>	<i>max-range</i>
50 node	87.2	109	118	107	93.0	136
60 node	78.4	98.0	112	93.0	88.0	123
70 node	71.6	89.5	100	86.0	79.0	112
80 node	68.0	85.0	94.0	80.0	75.0	106
90 node	64.8	81.0	87.0	77.0	69.1	101
100 node	61.6	77.0	84.0	74.0	65.2	96.3
110 node	59.2	74.0	80.2	73.2	64.1	92.5
120 node	56.8	71.0	78.1	73.0	63.0	88.8
130 node	54.4	68.0	75.0	70.0	59.0	85.0
140 node	52.8	66.0	74.2	68.0	56.0	82.5
150 node	51.2	64.0	71.5	61.1	55.1	80.0
160 node	49.6	62.0	69.0	59.8	55.2	77.5
170 node	48.0	60.0	66.0	57.0	53.6	75.0
180 node	46.8	58.5	64.1	56.0	52.1	73.1
190 node	46.0	57.5	62.0	53.0	50.5	71.9
200 node	45.6	57.0	60.9	52.7	50.0	71.3
210 node	45.3	56.6	58.1	52.0	48.2	70.8
220 node	45.0	56.2	57.6	50.3	47.6	70.3
230 node	44.6	55.8	56.2	49.0	47.5	69.8
240 node	44.3	55.4	55.1	48.0	46.5	69.3
250 node	44.0	55.0	52.7	47.4	46.4	68.8

In second experiment, the average number of neighbors and the number of links for PSOTC, RAA-2L, RAA-3L and HOM protocols is measured. The purpose of this experiment is to evaluate the ability of the proposed protocol to decrease the number of

neighbors. The result of this experiment is depicted in Fig. 3, Fig. 4, Table 4 and Table 5. As can be seen, the average number of neighbors and the number of links in the PSOTC is less than other protocols. Note that number of neighbors has a direct effect on interference between nodes and so, lower number of neighbors is better. Decreasing of the neighbors directly results in the decreation of the transition radius. But note that the decreation of the neighbors and also the transition radius is useful if the network connectivity is not removed. This problem will be evaluated accurately in next experiment.

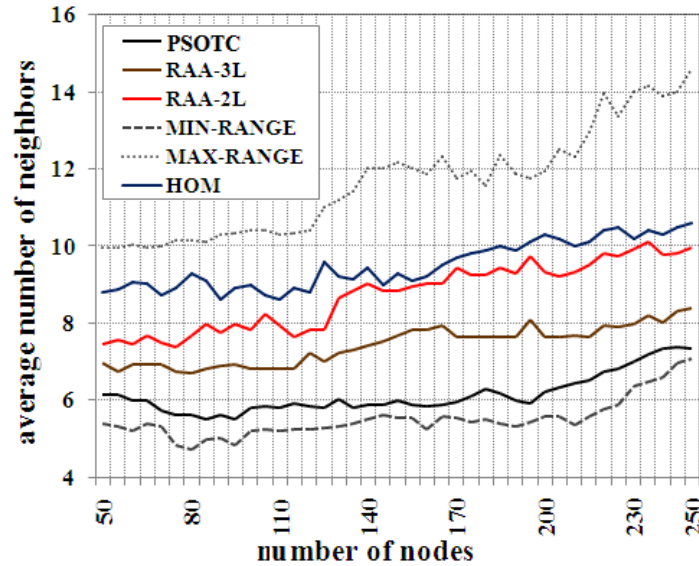


Figure 3. The average number of neighbors

Table 4. The average number of neighbors

Number of nodes (N)	<i>min-range</i>	<i>HOM</i>	<i>RAA-2L</i>	<i>RAA-3L</i>	<i>PSOTC</i>	<i>max-range</i>
50 node	5.40	8.80	7.45	6.95	6.12	9.96
60 node	5.20	9.05	7.46	6.93	6.00	10.02
70 node	5.30	8.71	7.47	6.92	5.72	10.01
80 node	4.71	9.30	7.68	6.71	5.60	10.14
90 node	5.02	8.60	7.76	6.90	5.60	10.30
100 node	5.20	9.00	7.83	6.82	5.79	10.42
110 node	5.20	8.60	7.92	6.83	5.81	10.30
120 node	5.24	8.80	7.84	7.22	5.83	10.42
130 node	5.30	9.20	8.63	7.24	6.01	11.20
140 node	5.50	9.42	9.01	7.40	5.89	12.02
150 node	5.53	9.30	8.83	7.66	6.00	12.16
160 node	5.23	9.20	9.04	7.83	5.85	11.86
170 node	5.53	9.70	9.43	7.62	5.95	11.76
180 node	5.50	9.90	9.23	7.64	6.27	11.56
190 node	5.33	9.90	9.30	7.65	5.97	11.86
200 node	5.57	10.3	9.31	7.64	6.22	11.95
210 node	5.37	10.0	9.32	7.66	6.42	12.30
220 node	5.77	10.4	9.80	7.92	6.72	13.95
230 node	6.37	10.2	9.91	7.99	7.00	14.00
240 node	6.57	10.3	9.78	8.02	7.32	13.90
250 node	7.09	10.6	9.94	8.39	7.33	14.61

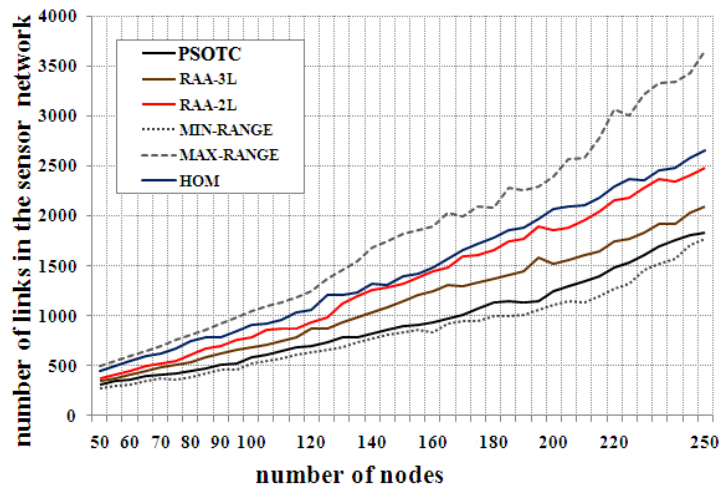


Figure 4. The number of links in the sensor networks

Table 5. The number of links in the sensor networks

Number of nodes (N)	<i>min-range</i>	<i>HOM</i>	<i>RAA-2L</i>	<i>RAA-3L</i>	<i>PSOTC</i>	<i>max-range</i>
50 node	270	440	373	348	306	498
60 node	312	543	448	416	360	601
70 node	371	610	523	484	400	701
80 node	377	744	614	537	448	811
90 node	452	774	698	621	504	927
100 node	520	900	783	682	579	1042
110 node	572	946	871	751	639	1133
120 node	629	1056	941	866	700	1250
130 node	689	1196	1122	941	781	1456
140 node	770	1319	1261	1036	824	1683
150 node	830	1395	1325	1149	900	1824
160 node	837	1472	1446	1253	936	1898
170 node	940	1649	1603	1295	1012	1999
180 node	990	1782	1661	1375	1129	2081
190 node	1013	1881	1767	1454	1134	2253
200 node	1114	2060	1863	1528	1244	2390
210 node	1128	2100	1958	1609	1348	2583
220 node	1270	2288	2156	1742	1478	3069
230 node	1466	2346	2280	1838	1610	3220
240 node	1577	2472	2347	1925	1757	3336
250 node	1773	2650	2485	2098	1833	3654

In the last experiment, the network connectivity in PSOTC is measured and compared to RAA-2L, RAA-3L and HOM protocols. As mentioned before, in these experiments, we suppose N_d is equal to 100. The probability of the complete connectivity is depicted in Fig. 5 and Table 6. As can be seen in Fig. 5 and Table 6, the probability of complete connectivity for PSOTC, RAA-2L, RAA-3L and MAX-RANGE are almost equal. So, the network connectivity in our protocol is acceptable.

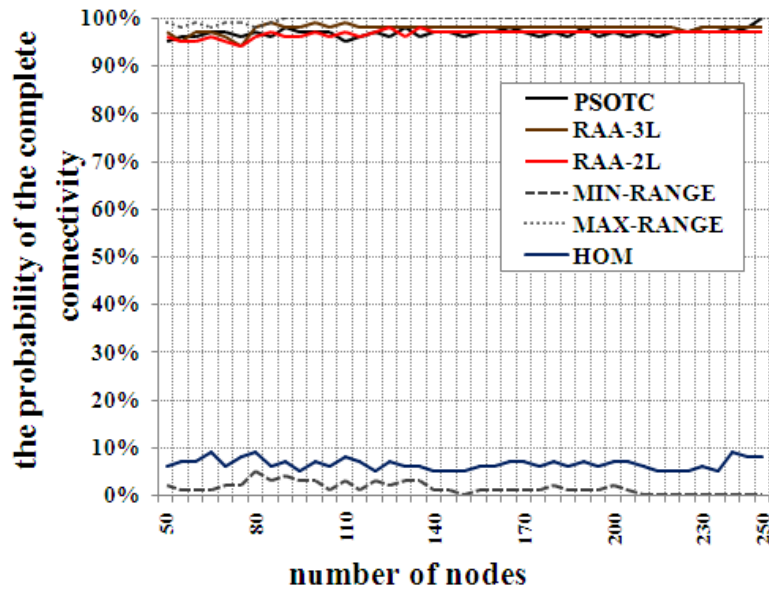


Figure 5. The probability of the complete connectivity

Table 6. The probability of the complete connectivity

Number of nodes (N)	<i>min-range</i>	<i>HOM</i>	<i>RAA-3L</i>	<i>RAA-3L</i>	<i>PSOTC</i>	<i>max-range</i>
50 node	0.02	0.06	0.96	0.97	0.95	0.99
60 node	0.01	0.07	0.96	0.97	0.96	0.99
70 node	0.02	0.06	0.95	0.96	0.97	0.99
80 node	0.05	0.09	0.96	0.98	0.97	0.98
90 node	0.04	0.07	0.96	0.98	0.98	1.00
100 node	0.03	0.07	0.97	0.99	0.97	1.00
110 node	0.03	0.08	0.97	0.99	0.95	1.00
120 node	0.03	0.05	0.97	0.98	0.97	1.00
130 node	0.03	0.06	0.96	0.98	0.98	1.00
140 node	0.01	0.05	0.97	0.98	0.97	1.00
150 node	0.00	0.05	0.97	0.98	0.96	1.00
160 node	0.01	0.06	0.97	0.98	0.97	1.00
170 node	0.01	0.07	0.96	0.98	0.97	1.00
180 node	0.02	0.07	0.97	0.97	0.97	1.00
190 node	0.01	0.06	0.97	0.98	0.98	1.00
200 node	0.02	0.07	0.97	0.98	0.97	1.00
210 node	0.00	0.06	0.96	0.98	0.97	1.00
220 node	0.00	0.05	0.97	0.98	0.97	1.00
230 node	0.00	0.06	0.97	0.97	0.98	1.00
240 node	0.00	0.09	0.98	0.98	0.97	1.00
250 node	0.00	0.08	0.97	0.98	0.99	1.00

5.3. Observations

The sample of the sensor nodes deployment is shown in Fig. 6. As can be seen in Fig. 6, while nodes have the minimum transition radius (R_{min}), the state of the network connectivity is very undesirable. Also while the nodes have maximum transition radius (R_{max}), the number of network links are lot such a way that not only the energy consumption is very high but also the collision within transition radius is lot.

These results can show the prominence of our proposed protocol. While maintaining network connectivity, it could decrease the average of transition radius and the average number of neighbor nodes. Thus it decreases the energy consumption and the interference between sensor nodes. PSOTC protocol has some advantages compared to

the previous protocols. PSOTC protocol dynamically adjusts the transition radius of the nodes (unlike previous protocols which should select radius values among predefined values). Thus, our protocol has the less average number of neighbors compared to the existing protocols. Also, the energy consumption in our protocol is less than others and the network lifetime will be prolonged. In addition, the network connectivity in our protocol is in the acceptable level.

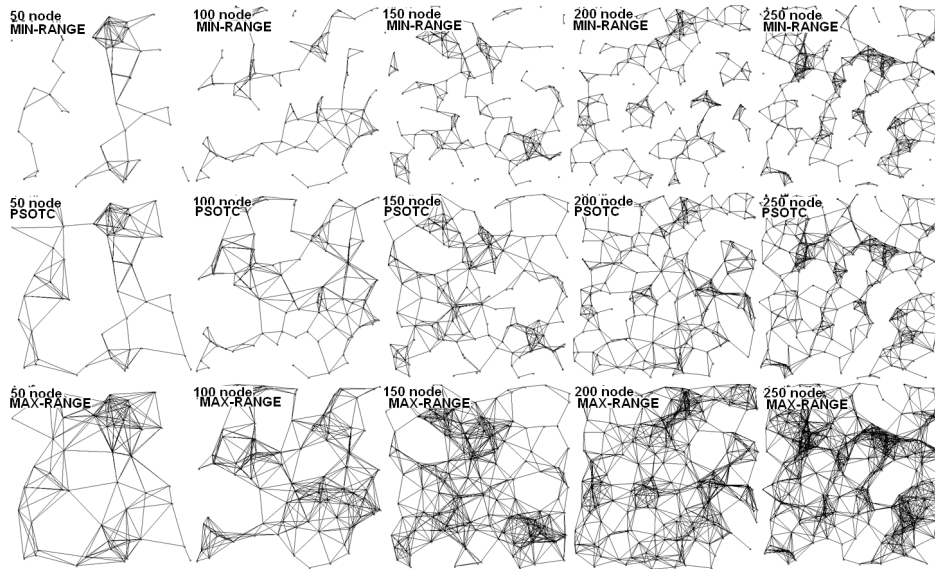


Figure 6. Topology control of the networks with different number of nodes using MIN-RANGE, PSOTC, and MAX-RANGE protocols

6. Conclusions

In this paper, we proposed a topology control protocol based on the PSO algorithm. In this protocol, the nodes can select a proper transition radius. Unlike previous protocols, the proposed protocol dynamically adjusts transition radius of nodes. The average of transition radius and the average number of neighbors in the proposed protocol is less than other protocols. So, the energy consumption in our protocol is lower than the other protocols and the network lifetime will be prolonged. In addition, the network connectivity in our protocol is in the acceptable level. The proposed protocol is simulated and the above advantages are shown in the simulation results.

References

- [1] X. Li, Y. Mao, and Y. Liang, "A Survey on Topology Control in Wireless Sensor Networks," Proc. 10th International Conference on Control, Automation, Robotics and Vision, ICARCV, Hanoi, Vietnam, Dec. 2008.
- [2] J. Jia, J. Chen, G. Chang, Z. Tan, "Energy efficient coverage control in wireless sensor networks based on multi-objective genetic algorithm," Computers and Mathematics with Applications, vol. 57, no. 11, pp. 1756-1766, 2009.

- [3] X. Zhang, X. Ding, S. Lu, and G. Chen, "Principles for Energy-Efficient Topology Control in Wireless Sensor Networks," Proc. IEEE 5th International Conference on Wireless Communications, Networking and Mobile Computing (WiCOM '09), Beijing, China, Sept. 2009.
- [4] P. Santi, "Topology Control in Wireless Ad Hoc and Sensor Networks," ACM Computer Survey, vol. 37, no. 2, pp. 164-194, 2005.
- [5] V. Rodoplu, and T. H. Meng, "Minimum energy mobile wireless networks," IEEE Journal on Selected Areas in Communications, vol. 17, no. 8, pp. 1333-1344, Aug. 1999.
- [6] N. Li, J. Hou, and L. Sha., "Design and analysis of an MST-based topology control algorithm," IEEE Trans. Wireless Comm., vol. 4, no. 3, pp. 1195-1206, May 2005.
- [7] R. Wattenhofer, L. Li, P. Bahl and Y.M. Wang, "Distributed topology control for power efficient operation in multihop wireless ad hoc networks," Proc. IEEE 20th Annual Joint Conference of the IEEE Computer and Communications Societies, Anchorage, AK, USA, pp. 1388– 1397, April 2001.
- [8] R. Wattenhofer and A. Zollinger, "XTC: a practical topology control algorithm for ad-hoc networks," Proc. 18th International Parallel and Distributed Processing Symposium (IPDPS '04), Santa Fe, New Mexico, pp. 2-16, April 2004.
- [9] D. Blough, M. Leoncini, G. Resta., and P. Santi, "The k-neighbors protocol for symmetric topology control in ad hoc networks," Proc. ACM MobiHoc'03, Annapolis, Maryland, USA, pp. 141-152, June 2003.
- [10] A. Venuturumilli, A. Minai, "Obtaining Robust Wireless Sensor Networks Through Self-Organization of Heterogeneous Connectivity," Proc. International Conference on Complex Systems (ICCS'06), Boston, MA, June 2006.
- [11] S. M. Jameii, A. Nikdel, A. M.Bidgoli, "GATC: A new Genetic Algorithm-based Topology Control Protocol for Wireless Sensor Networks," Proc. International Conference on Intelligent Network and Computing (ICINC), Kuala Lumpur, Malaysia, pp. 365-369, Nov. 2010.
- [12] D. Stauffer, A. Aharony, Introduction to Percolation Theory, Taylor & Francis, London, 1994.
- [13] J. Jia, J. Chen, G. Chang, Y. Wen, J. Song, "Multi-objective optimization for coverage control in wireless sensor network with adjustable sensing radius,"Computers and Mathematics with Applications, vol.57, no. 11, pp. 1767-1775, 2009.
- [14] J. Jia, J. Chen, Y. Wen, G. Chang, "An extensible core-control routing protocol in large scale ad-hoc networks," Proc. 6th International Conference on ITS Telecommunications, Chengdu, China, pp. 955-958, June 2006.
- [15] M. Lu, J. Wu, M. Cardei, and M. Li, "Energy-efficient connected coverage of discrete targets in wireless sensor networks," Proc. International Conference on Computer Networks and Mobile Computing (ICCNMC 2005), Zhangjiajie, China, pp. 43-52, Aug. 2005.
- [16] N. Bulusu, J. Heidemann, D. Estrin, "GPS-less low-cost outdoor localization for very small devices", IEEE Personal Communications Magazine, vol. 7, no. 5, pp. 28-34, Oct. 2000.
- [17] S. Jardosh, P. Ranjan, "A Survey: Topology Control For Wireless Sensor Networks," Proc. International Conference on Signal processing, Communications and Networking (ICSCN '08), Chennai, India, pp. 422-427, Jan. 2008.

Authors



Arash Nikdel received the B.S. degree in Computer Engineering from the Islamic Azad University and the M.S. degrees in Computer Engineering from Ahvaz Science and Research Branch in Iran, in 2007 and 2011, respectively. His research interests include wireless sensor and Ad-hoc networks.



Mahdi Mosleh received his B.S. in computer engineering from Islamic Azad University, Dezful Branch, in 2008 and the M.S. in computer engineering from Islamic Azad University, Dezful, in 2011 in computer engineering. His research interests are Wireless Sensor Network, Audio and Image watermarking.



Hagar Noori received the B.S. degree in Computer Engineering from the Islamic Azad University and the M.S. degrees in Computer Engineering from Arak Science and Research Branch in Iran, in 2007 and 2012, respectively. Her research interests include wireless sensor and Ad-hoc networks.